

# Searching for the lost Unicorn: a prominent feature in the radial velocity distribution of stars in Vela from *Gaia* DR2 data

R. de la Fuente Marcos<sup>1</sup><sup>\*</sup> and C. de la Fuente Marcos<sup>2</sup>

<sup>1</sup>*AEGERA Research Group, Facultad de Ciencias Matemáticas, Universidad Complutense de Madrid, Ciudad Universitaria, E-28040 Madrid, Spain*

<sup>2</sup>*Universidad Complutense de Madrid, Ciudad Universitaria, E-28040 Madrid, Spain*

Accepted 2018 August 29. Received 2018 August 29; in original form 2018 July 8

## ABSTRACT

Stellar streams are ubiquitous in the Galactic halo and they can be used to improve our understanding of the formation and evolution of the Milky Way as a whole. The so-called Monoceros Ring might have been the result of satellite accretion. Guglielmo et al. have used  $N$ -body simulations to search for the progenitor of this structure. Their analysis shows that, if the Ring has a dwarf galaxy progenitor, it might be found in the background of one out of eight specific areas in the sky. Here, we use *Gaia* DR2 data to perform a systematic exploration aimed at confirming or rejecting this remarkable prediction. Focusing on the values of the radial velocity to uncover possible multimodal spreads, we identify a bimodal Gaussian distribution towards Galactic coordinates  $(l, b) = (271^\circ, +2^\circ)$  in Vela, which is one of the locations of the progenitor proposed by Guglielmo et al. This prominent feature with central values  $60 \pm 7 \text{ km s}^{-1}$  and  $97 \pm 10 \text{ km s}^{-1}$ , may signal the presence of the long sought progenitor of the Monoceros Ring, but the data might also be compatible with the existence of an unrelated, previously unknown, kinematically coherent structure.

**Key words:** methods: statistical – celestial mechanics – Galaxy: disc – Galaxy: evolution – Galaxy: stellar content – Galaxy: structure.

## 1 INTRODUCTION

Beyond the nominal edge of the Milky Way disc, 15 kpc from the Galactic centre, lies a complex network of coherent stellar structures whose origins are not yet fully understood (see e.g. Schlaufman 2011; Xue et al. 2011; Pila Díez 2015; Smith 2016). Some may be the result of the Milky Way cannibalizing nearby dwarf galaxies (Ibata, Gilmore & Irwin 1994), others could be just stellar lumps induced by the combined action of the gravitational potential of the Galaxy and those of passing and/or falling neighbours (Xu et al. 2015; Schönrich & Dehnen 2018). The study of these structures can help in understanding how the Milky Way came into existence and how it has evolved progressively to become what we observe now. Among all these structures, the true nature of the so-called Monoceros Ring remains elusive. Originally identified by Newberg et al. (2002), the structure is considered by some as a *bona fide* stellar stream (e.g. Ibata et al. 2003; Yanny et al. 2003; Conn et al. 2007; Grillmair, Carlin & Majewski 2008; Ivezić et al. 2008; Michel-Dansac et al. 2011; Sollima et al. 2011; Laporte et al. 2018), while others put its origin in the (flared thick) disc of the Milky Way (e.g. Carraro et al. 2005; Momany et al. 2006; Kalberla et al. 2014; López-Corredoira & Molgó 2014; Sheffield et al. 2018; Wang et al. 2018). Alternative scenarios put its provenance in an outer spiral arm such as the one described by

Dame & Thaddeus (2011) or in undulations of the disc (Li et al. 2017) like those discussed by Xu et al. (2015).

Guglielmo et al. (2018) have recently explored the kinematics, proper motions, and the nature of the putative progenitor of the Monoceros Ring. Although they could not confirm that the Ring has its origin in an accretion episode, their analysis argues that, if the Ring has a dwarf galaxy progenitor, it might be found in the background of one out of eight well-defined areas in the sky. Here, we use *Gaia* DR2 data to perform a systematic exploration of these areas aimed at confirming or rejecting their prediction, focusing on the values of the radial velocity to uncover possible multimodal distributions. This Letter is organized as follows. Section 2 presents the input data and tools used in our analysis. The eight radial velocity distributions are explored in Section 3. Section 4 presents the analysis of a bimodal Gaussian distribution found towards Galactic coordinates  $(l, b) = (271^\circ, +2^\circ)$  in Vela. In Section 5, we study the statistical significance of our findings. Results are discussed in Section 6 and conclusions are summarized in Section 7.

## 2 INPUT DATA AND TOOLS

Guglielmo et al. (2018) have proposed that, if the Monoceros Ring has a dwarf galaxy progenitor, it might be found towards one out of eight patches of sky. In their fig. 2, three patches are linked to their Model 2, two to their Model 3, and three more to their Model 4.

\* E-mail: rauldefuentemarcos@ucm.es

Model 2 predicts a progenitor located in the range of Galactocentric distances,  $d$ ,  $27\pm 12$  kpc. Model 3 predictions are for the range  $40\pm 12$  kpc, and those from Model 4 span the range  $31\pm 13$  kpc. Model 2 indicates three possible locations centred at Galactic coordinates  $(l, b)$  of  $(14^\circ, -1^\circ)$  in the constellation of Sagittarius (henceforth Model 2 A),  $(352^\circ, -2^\circ)$  in Scorpius (Model 2 B), and  $(232^\circ, +2^\circ)$  in Puppis (Model 2 C); Model 3 gives  $(11^\circ, -2^\circ)$  in Sagittarius (Model 3 A) and  $(354^\circ, -1^\circ)$  in Scorpius (Model 3 B); Model 4 suggests  $(17^\circ, -2^\circ)$  in Scutum (Model 4 A),  $(249^\circ, -1^\circ)$  in Puppis (Model 4 B), and  $(271^\circ, +2^\circ)$  in Vela (Model 4 C). Our objective is to analyse data in a three-dimensional sub-space (eight of them) constrained by the values of  $l$ ,  $b$  and  $d$  in Guglielmo et al. (2018).

*Gaia* DR2 (Gaia Collaboration 2016, 2018a) provides extensive astrometric and photometric data —namely, coordinates, parallax, radial velocity, proper motions, blue, red and green magnitudes, and their respective standard errors— that can be used to perform the exploration required to confirm or reject the prediction made by Guglielmo et al. (2018). Out of 87 733 672 sources with strictly positive values of the parallax, we found 4 831 766 sources with values of the radial velocity,  $V_r$ . This is our primary sample and we have been able to extract 475, 878, 102, 252, 247, 344, 199, and 150 sources, respectively, for the eight patches of sky singled out by Guglielmo et al. (2018). The extraction process has been restricted to a square region of side  $10^\circ$ , centred at the proposed locations; i.e. for Model 2 A, the ranges in  $l$  and  $b$  are, respectively,  $(9^\circ, 19^\circ)$  and  $(-6^\circ, +4^\circ)$  with distances within  $27\pm 12$  kpc. We believe that the size of our sampling window is large enough to obtain robust results (see fig. 2 in Guglielmo et al. 2018).

When needed and following the approach outlined by Johnson & Soderblom (1987), we have used the input data to compute Galactic space velocities and their uncertainties in a right-handed coordinate system for  $U$ ,  $V$ , and  $W$ ; axes are positive in the directions of the Galactic centre, Galactic rotation, and the North Galactic Pole (NGP). The Galactocentric standard of rest is a right-handed coordinate system centred at the Galactic centre. Axes are positive in the directions of the Sun, Galactic rotation, and the NGP. The necessary values of the Solar motion were taken from Schönrich, Binney & Dehnen (2010). Averages, standard deviations, medians, interquartile ranges (IQRs) and other statistical parameters have been computed in the usual way (see e.g. Wall & Jenkins 2012)

### 3 VELOCITY DISTRIBUTIONS

Fig. 1 shows the radial velocity distributions of the eight *Gaia* DR2 samples associated with the possible locations of the progenitor of the Monoceros Ring discussed by Guglielmo et al. (2018). The histograms displayed here have a statistically meaningful bin width computed using the Freedman-Diaconis rule (Freedman & Diaconis 1981), i.e.  $2 \text{ IQR } n^{-1/3}$ , where  $n$  is the number of sources; cumulative frequencies are plotted as dashed curves. The values of the IQRs (median values in parentheses) in  $\text{km s}^{-1}$  are, respectively (top to bottom in Fig. 1), 110.27 (+31), 134.93 (−56.98), 32.51 (+105.22), 127.33 (+15.82), 138.47 (−58.01), 99.33 (+31.83), 32.99 (+106.14), and 44.56 (+75.78), and the bin sizes of the associated histograms are, respectively (also in  $\text{km s}^{-1}$ ), 28.26, 28.18, 13.92, 40.31, 44.14, 28.35, 11.30, and 16.77. Given the fact that the values of the IQRs for the different regions are quite different, our analysis is sensitive to finding kinematically cold substructures only in a few of them.

As the Galactic latitude of the various samples corresponds to

the disc, the presence of a single peak in the radial velocity distribution can be interpreted as the signature of a disc-like population; if additional peaks are found, they may correspond to coherent structures different from the disc. As a reference, the solid lines in Fig. 1 show the distributions of synthetic samples of field stars generated from the GALAXIA<sup>1</sup> model (Sharma et al. 2011) within one square degree around the region’s centre (thin red curve, entire synthetic sample, thick black curve, synthetic sample with Galactocentric distance  $> 15$  kpc, normalized to the peak of the corresponding histogram). In general and with the exception of the sample of location C of Model 4 in Guglielmo et al. (2018) —see Fig. 1, bottom panel— it is not possible to identify any statistically significant bimodal behaviour. The error bars in the bottom panel of Fig. 1 have been calculated using Poisson statistics ( $\sigma = \sqrt{n}$ ) and applying the approximation given by Gehrels (1986) when  $n < 21$ ,  $\sigma \sim 1 + \sqrt{0.75 + n}$ .

### 4 A BIMODAL DISTRIBUTION OF RADIAL VELOCITIES IN VELA

The bottom panel in Fig. 1 seems to follow a bimodal Gaussian distribution produced by populations with central velocities  $60\pm 7 \text{ km s}^{-1}$  and  $97\pm 10 \text{ km s}^{-1}$  and consistent dispersions of about  $10 \text{ km s}^{-1}$ . Assuming that the observed distribution is mainly the sum of two normal distributions, the bimodality index (difference of means divided by dispersion) is 3.7, and the ratio of the two populations is nearly 1:1. We interpret the population with the lowest central velocity as an extension of the thin disc at average Galactocentric distances close to 30 kpc. This interpretation appears to be compatible with predictions from GALAXIA, but the higher  $V_r$  peak is neither compatible with the thin disc (thin curve) nor with the halo component (thick curve), which should have values close to  $150 \text{ km s}^{-1}$ . Fig. 2 shows that both populations (low velocity in green, high velocity in red) have similar distributions in terms of proper motions ( $\mu_\alpha \cos \delta$ ,  $\mu_\delta$ ), although the high-velocity group exhibits a larger dispersion in the values of their proper motions in right ascension —averages, standard deviations, medians, and IQRs are (disc members)  $-3.9\pm 0.7 \text{ mas yr}^{-1}$ ,  $-3.78 \text{ mas yr}^{-1}$ ,  $0.77 \text{ mas yr}^{-1}$  (right ascension),  $3.2\pm 0.8 \text{ mas yr}^{-1}$ ,  $3.19 \text{ mas yr}^{-1}$ ,  $0.88 \text{ mas yr}^{-1}$  (declination), and (higher  $V_r$  peak)  $-3.8\pm 1.1 \text{ mas yr}^{-1}$ ,  $-3.73 \text{ mas yr}^{-1}$ ,  $1.24 \text{ mas yr}^{-1}$  (right ascension),  $3.3\pm 0.9 \text{ mas yr}^{-1}$ ,  $3.24 \text{ mas yr}^{-1}$ ,  $1.11 \text{ mas yr}^{-1}$  (declination). As the values of their distances span the same range —averages, standard deviations, medians, and IQRs for the parallaxes are (disc)  $0.039\pm 0.009 \text{ mas}$ ,  $0.039 \text{ mas}$ ,  $0.018 \text{ mas}$ , and (higher  $V_r$  peak)  $0.040\pm 0.011 \text{ mas}$ ,  $0.040 \text{ mas}$ ,  $0.019 \text{ mas}$ — their tangential velocities are also similar. The colour-magnitude diagram in Fig. 3 displays the intrinsic values (i.e. corrected for extinction and reddening using the data provided by *Gaia* DR2) of these two populations, which follow similar distributions made of probable young stars, perhaps classical Cepheids, although the high-velocity population seems to be slightly older and/or have different metallicity. Fig. 3 is similar to figs 19b and 20 in Andrae et al. (2018) in which the red giant branch (RGB) corresponds to an age of 1–2 Gyr. As a reference, three 50 Myr and one 1.5 Gyr PARSEC v1.2S + COLIBRI PR16<sup>2</sup> isochrones are also plotted. Most sources in the higher  $V_r$  peak of the bottom panel of Fig. 1 are too bright to be RGB stars.

<sup>1</sup> <http://www.physics.usyd.edu.au/~sanjib/code/>

<sup>2</sup> <http://stev.oapd.inaf.it/cgi-bin/cmd>

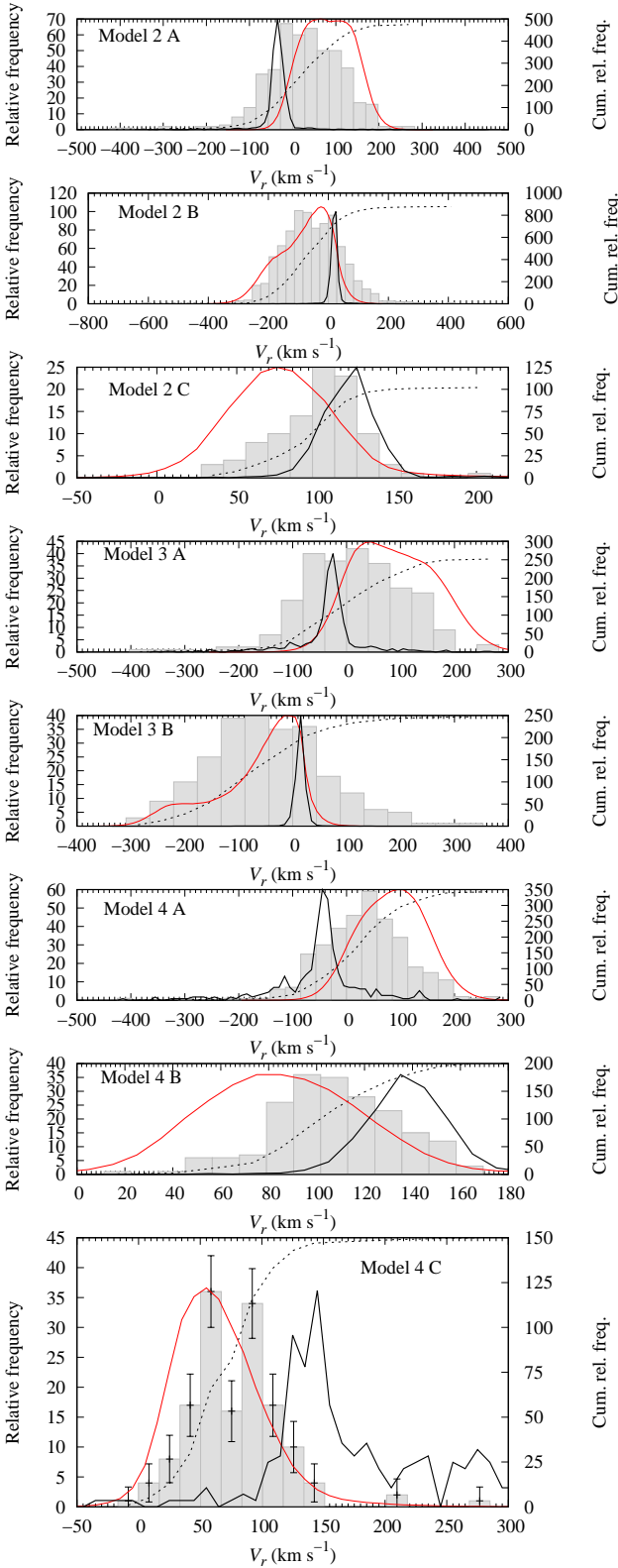


**Figure 1.** Radial velocity distributions of the *Gaia* DR2 samples associated with the eight possible progenitor locations of the Monoceros Ring discussed in [Guglielmo et al. \(2018\)](#). Solid line distributions from GALAXIA ([Sharma et al. 2011](#)) with warp and flare. See the text for details.

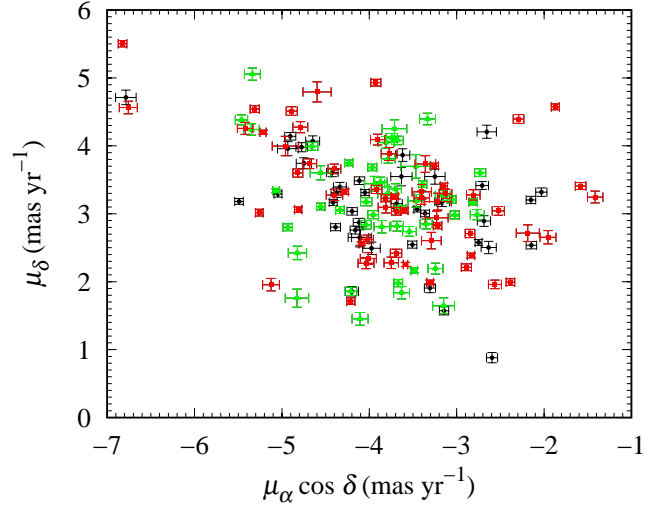


**Figure 2.** Proper motion components with  $1\sigma$  error bars for the *Gaia* DR2 sample of location C of Model 4 in [Guglielmo et al. \(2018\)](#): green triangles, stars assumed to be part of the disc ( $45 \text{ km s}^{-1} < V_r < 75 \text{ km s}^{-1}$ ), red squares, stars linked to the high-velocity peak in the bottom panel of Fig. 1 ( $80 \text{ km s}^{-1} < V_r < 120 \text{ km s}^{-1}$ ), others plotted as black circles.

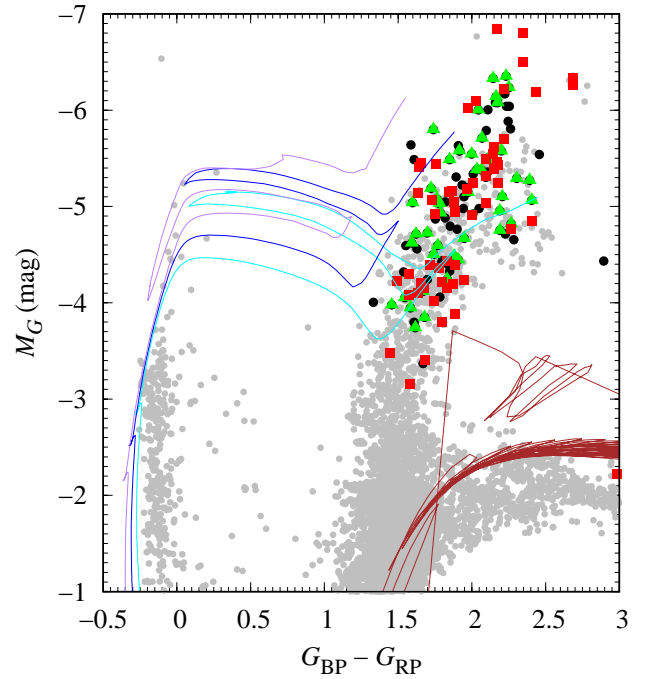


**Figure 3.** Colour-magnitude diagram for the same sample in Fig. 2, similar to fig. 5 in [Gaia Collaboration \(2018b\)](#). The entire *Gaia* DR2 sample of location C of Model 4 is plotted in light grey. Three isochrones of an age of 50 Myr and solar (cyan), solar/5 (blue), and solar/50 (purple) metallicities and one of an age of 1.5 Gyr (brown) and solar metallicity from [Marigo et al. \(2017\)](#) are plotted as a reference.

## 5 STATISTICAL SIGNIFICANCE

Fig. 1, bottom panel, shows that the sample from Model 4 C is bimodal with central values  $60 \pm 7 \text{ km s}^{-1}$  and  $97 \pm 10 \text{ km s}^{-1}$ . The separation between the peaks is  $34 \text{ km s}^{-1}$ , which is of order of IQR and well above the usual values of the uncertainties in the values of the radial velocities (well below  $5 \text{ km s}^{-1}$  in most cases,

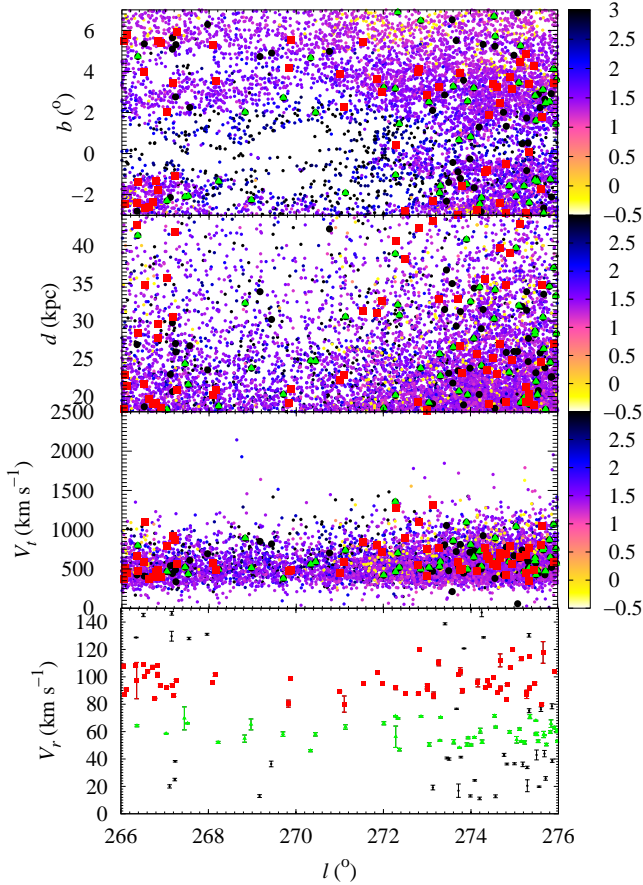


**Figure 4.** Distribution in Galactic coordinates (top panel), distance (second to top panel), and tangential velocity (second to bottom panel) for the entire *Gaia* DR2 sample of location C of Model 4 in [Guglielmo et al. \(2018\)](#). The colour map shows the value of the colour index in [Fig. 3](#), computed as shown in [Gaia Collaboration \(2018b\)](#). Hot stars appear lighter in colour and cold stars darker. Points in green and red as in [Figs 2 and 3](#). The radial velocity distribution with error bars is shown in the bottom panel.

see [Fig. 4](#), bottom panel). The difference between the bin centred at  $58.7 \text{ km s}^{-1}$  and the one at  $75.5 \text{ km s}^{-1}$  is nearly  $4\sigma$ ; in addition, the excess of the bin centred at  $92.2 \text{ km s}^{-1}$  with respect to the one at  $75.5 \text{ km s}^{-1}$  is about  $3.5\sigma$ —in both cases using the  $\sigma$ -value at the dip. If we repeat the same analysis for Model 2 B ([Fig. 1](#), second to top panel), the single other that might exhibit signs of bimodality, excesses of just  $1.1\sigma$  are found.

## 6 DISCUSSION

In general, the data from *Gaia* DR2 for sources beyond 15 kpc are affected by large uncertainties, particularly large in the case of the parallax values (i.e. distances). Our main findings are based on a parameter, the value of the radial velocity, which is definitely the least uncertain of the data set, if measured. The samples used in this investigation have very good values of the radial velocity and also the proper motions, but the values of the distances derived from the parallaxes are rather uncertain. The values of the tangential velocities and absolute magnitudes inherit these large errors. Therefore, our conclusions must be based on the value of the radial velocity and those of the components of the proper motion. These are sufficiently reliable.

It may be argued that both peaks in the distribution of radial velocity in [Fig. 1](#), bottom panel, could be the result of the presence of small, distant, and decaying clusters such as E 3 ([de la Fuente Marcos et al. 2015](#)). In such cases, we should observe very small concentrations of relevant sources. [Fig. 4](#), top panel, shows the distribution of low- and high-velocity sources in Galactic coordinates and no such obvious concentrations are observed. The same can be said about the values of the distance in [Fig. 4](#), second to top panel. In [Fig. 4](#), both the sample with radial velocities and the most general one are plotted using the intrinsic colour index in [Fig. 3](#) as third coordinate. [Fig. 4](#), top panel, clearly indicates that the effects of extinction are very important in this region with the empty spaces corresponding to putative missing sources not present in *Gaia* DR2 because the foreground population and associated gas clouds effectively block the light from these sources. The fact that the sources surrounding the empty spaces tend to have the largest reddening values, clearly confirms that reddening is a major concern here. It is however unlikely that the dominant role that interstellar extinction indeed has in this region may have a major impact on our conclusions, which are based on the distribution of radial velocities for the most part. [Fig. 4](#), second to bottom panel, shows the values of the tangential velocity,  $V_t$ , which exhibit a considerable spread due to the large uncertainties in the values of the distances.

[Fig. 5](#) makes the issue of the uncertainties in the values of the distance explicit. In general, the Galactocentric velocity components have very large error bars and this makes it virtually impossible to disentangle the two structures that may contribute to the bimodal radial velocity distribution observed in [Fig. 1](#), bottom panel. The prominent feature with central value  $97 \pm 10 \text{ km s}^{-1}$ , may signal the presence of the long sought progenitor of the Monoceros Ring, but the data might also be compatible with the existence of an unrelated, previously unknown, kinematically coherent structure, such as a distant spiral arm or a spur that connects two well-separated arms. In [Fig. 4](#), top panel, the distribution above the disc looks quite stream-like, as opposed to cluster-like. The location in the sky of structure B in [fig. 5](#) of [Martin et al. \(2004\)](#) matches somehow that of the feature discussed here, but the distance range appears to be different. The same can be said about the Argo structure discussed by [Rocha-Pinto et al. \(2006\)](#).

## 7 CONCLUSIONS

In this Letter, we have investigated the plausibility of the predictions made by [Guglielmo et al. \(2018\)](#) regarding the possible location of the putative progenitor of the Monoceros Ring using data from *Gaia* DR2 and focusing on the distribution of radial velocities. A statistically robust feature in the radial velocity distribution of stars in Vela has been identified. Our conclusions are:

- (i) Based on the distributions of radial velocities provided by *Gaia* DR2, the distant stellar populations located in the regions proposed by [Guglielmo et al. \(2018\)](#) appear to be compatible with single populations (i.e. no kinematically heterogeneous samples) in all but one case, that of the region towards the constellation of Vela.
- (ii) We have identified a statistically significant bimodal Gaussian distribution towards Galactic coordinates  $(l, b) = (271^\circ, +2^\circ)$ , which is one of the present-day locations of the progenitor of the Monoceros Ring proposed by [Guglielmo et al. \(2018\)](#). This feature has central values of the radial velocity of  $60 \pm 7 \text{ km s}^{-1}$  and  $97 \pm 10 \text{ km s}^{-1}$ .

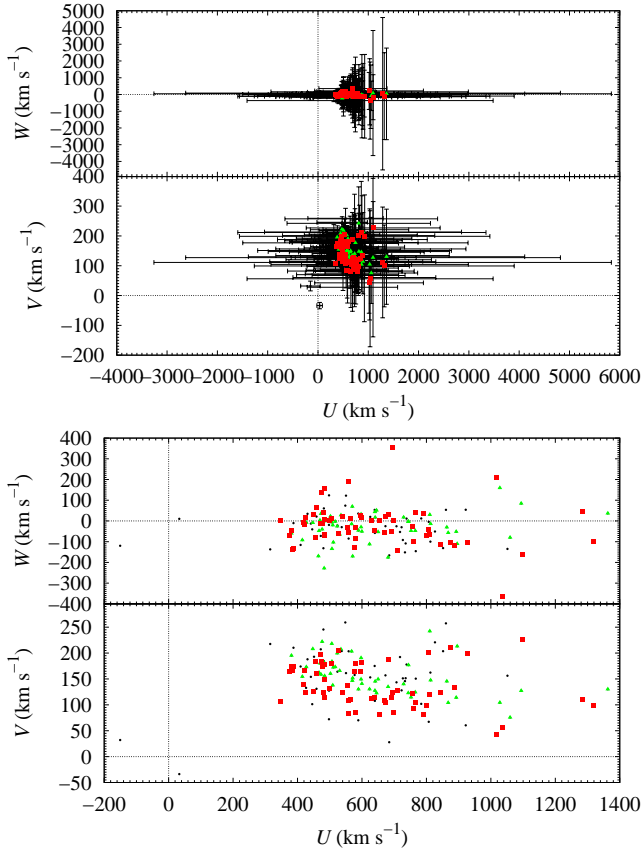


**Figure 5.** Galactocentric velocity components with (top two panels) and without error bars (bottom two panels). Triangles in green and squares in red as in Figs 2–4.

- (iii) The prominent feature found towards Vela may signal the presence of the long sought progenitor of the Monoceros Ring, but the data might also be compatible with the existence of an unrelated, previously unknown, kinematically coherent structure.
- (iv) Interstellar extinction may be a major obstacle to disentangle the true nature of the two remote populations that appear to share the patch of sky around  $(l, b) = (271^\circ, +2^\circ)$ .

## ACKNOWLEDGEMENTS

We thank the anonymous referee for a particularly insightful and constructive review, and A. I. Gómez de Castro for comments and for providing access to computing facilities; RdIFM thanks L. Beitia-Antero for extensive discussions on *Gaia* DR2 data. This work was partially supported by the Spanish MINECO under grant ESP2015-68908-R. In preparation of this Letter, we made use of the NASA Astrophysics Data System, the ASTRO-PH e-print server, and the SIMBAD and VizieR databases operated at CDS, Strasbourg, France. This work has made use of data from the European Space Agency (ESA) mission *Gaia* (<https://www.cosmos.esa.int/gaia>), processed by the *Gaia* Data Processing and Analysis Consortium (DPAC, <https://www.cosmos.esa.int/web/gaia/dpac/consortium>). Funding for the DPAC has been provided by national institutions, in particular the institutions participating in the *Gaia* Multilateral Agreement.

## REFERENCES

- Andrae R. et al., 2018, *A&A*, 616, A8  
 Carraro G., Vázquez R. A., Moitinho A., Baume G., 2005, *ApJ*, 630, L153  
 Conn B. C. et al., 2007, *MNRAS*, 376, 939  
 Dame T. M., Thaddeus P., 2011, *ApJ*, 734, L24  
 de la Fuente Marcos R., de la Fuente Marcos C., Moni Bidin C., Ortolani S., Carraro G., 2015, *A&A*, 581, A13  
 Freedman D., Diaconis P., 1981, *Z. Wahrscheinlichkeitstheor. verwandte Geb.*, 57, 453  
 Gaia Collaboration, 2016, *A&A*, 595, A1  
 Gaia Collaboration, 2018a, *A&A*, 616, A1  
 Gaia Collaboration, 2018b, *A&A*, 616, A10  
 Gehrels N., 1986, *ApJ*, 303, 336  
 Grillmair C. J., Carlin J. L., Majewski S. R., 2008, *ApJ*, 689, L117  
 Guglielmo M., Lane R. R., Conn B. C., Ho A. Y. Q., Ibata R. A., Lewis G. F., 2018, *MNRAS*, 474, 4584  
 Ibata R. A., Gilmore G., Irwin M. J., 1994, *Nature*, 370, 194  
 Ibata R. A., Irwin M. J., Lewis G. F., Ferguson A. M. N., Tanvir N., 2003, *MNRAS*, 340, L21  
 Ivezić Ž. et al., 2008, *ApJ*, 684, 287  
 Johnson D. R. H., Soderblom D. R., 1987, *AJ*, 93, 864  
 Kalberla P. M. W., Kerp J., Dedes L., Haud U., 2014, *ApJ*, 794, 90  
 Laporte C. F. P., Gómez F. A., Besla G., Johnston K. V., Garavito-Camargo N., 2018, *MNRAS*, 473, 1218  
 Li T. S. et al., 2017, *ApJ*, 844, 74  
 López-Corredoira M., Molgó J., 2014, *A&A*, 567, A106  
 Marigo P. et al., 2017, *ApJ*, 835, 77  
 Martín N. F., Ibata R. A., Bellazzini M., Irwin M. J., Lewis G. F., Dehnen W., 2004, *MNRAS*, 348, 12  
 Michel-Dansac L., Abadi M. G., Navarro J. F., Steinmetz M., 2011, *MNRAS*, 414, L1  
 Momany Y., Zaggia S., Gilmore G., Piotto G., Carraro G., Bedin L. R., de Angeli F., 2006, *A&A*, 451, 515  
 Newberg H. J. et al., 2002, *ApJ*, 569, 245  
 Pila Díez B., 2015, Ph.D. Thesis, Univ. Leiden  
 Rocha-Pinto H. J., Majewski S. R., Skrutskie M. F., Patterson R. J., Nakanishi H., Muñoz R. R., Sofue Y., 2006, *ApJ*, 640, L147  
 Schlaufman K. C., 2011, Ph.D. Thesis, Univ. California, Santa Cruz  
 Schönrich R., Dehnen W., 2018, *MNRAS*, 478, 3809  
 Schönrich R., Binney J., Dehnen W., 2010, *MNRAS*, 403, 1829  
 Sharma S., Bland-Hawthorn J., Johnston K. V., Binney J., 2011, *ApJ*, 730, 3  
 Sheffield A. A., Price-Whelan A. M., Tzanidakis A., Johnston K. V., Laporte C. F. P., Sesar B., 2018, *ApJ*, 854, 47  
 Smith M. C., 2016, *Tidal Streams in the Local Group and Beyond: Observations and Implications*. ASSL. Vol. 420, Springer International Publishing, Switzerland, p. 113  
 Sollima A., Valls-Gabaud D., Martínez-Delgado D., Fliri J., Peñarrubia J., Hoekstra H., 2011, *ApJ*, 730, L6  
 Wall J. V., Jenkins C. R., 2012, *Practical Statistics for Astronomers*. Cambridge Univ. Press, Cambridge  
 Wang H.-F., Liu C., Xu Y., Wan J.-C., Deng L., 2018, *MNRAS*, 478, 3367  
 Xu Y., Newberg H. J., Carlin J. L., Liu C., Deng L., Li J., Schönrich R., Yanny B., 2015, *ApJ*, 801, 105  
 Xue X.-X. et al., 2011, *ApJ*, 738, 79  
 Yanny B. et al., 2003, *ApJ*, 588, 824

This paper has been typeset from a  $\text{\TeX}/\text{\LaTeX}$  file prepared by the author.